

Persistent homology analysis for QCD effective models

Kouji Kashiwa,^{a,*} Takenori Hirakida^b and Hiroaki Kouno^c

^a*Fukuoka Institute of Technology, Wajiro, Fukuoka 811-0295, Japan*

^b*Izumi Chuo high school, Izumi 899-0213, Japan*

^c*Department of Physics, Saga University, Saga 840-8502, Japan*

E-mail: kashiwa@fit.ac.jp

The persistent homology analysis has been widely used to investigate the phase structure and the spatial structure based on the topological properties of the data space via the filtration of the simplicial complex. In this talk, I explained how to apply the persistent homology analysis to the QCD effective model with heavy quarks; i.e., the effective Polyakov-line model and the Potts model with the suitably tuned external magnetic field. In this proceedings, the Potts model results are mainly shown. It is shown that the averaged birth-death time ratio has the same information with the spatial averaged Polyakov-loop and the maximum birth-death time ratio has more information than the averaged birth-death time ratio. Then, the peak structure near the first-order phase transition point and the valley structure before the transition are clarified. In addition, the plateau behavior is found between the first-order transition and the crossover.

*The 38th International Symposium on Lattice Field Theory, LATTICE2021 26th-30th July, 2021
Zoom/Gather@Massachusetts Institute of Technology*

*Speaker

1. Introduction

Elucidating the nature of the phase structure of quantum chromodynamics (QCD) at finite temperature (T) and the real quark chemical potential (μ_R) is one of interesting and important subjects in elementary particle, hadron and nuclear physics. In the pure gauge limit where the quarks are not dynamical, the Polyakov loop respecting the gauge invariant holonomy perfectly characterizes the confinement-deconfinement transition; see Ref. [1]. In such case, the spontaneous breaking of the center (\mathbb{Z}_{N_c}) symmetry, where N_c is the number of colors, can describe the confinement-deconfinement phase transition and then the Polyakov loop becomes the order parameter of it. However, the Polyakov loop is no longer the order parameter in the system with dynamical quarks since the relation between the Polyakov loop and the one-quark excitation free energy is missed. Because of the above fact, the confinement-deconfinement nature of QCD with the realistic quark mass is still an open question; for example, see Ref. [2] for the recent proposed deconfinement scenario at finite μ_R .

There are several different approaches to investigate the confinement-deconfinement nature. One interesting approach is the topological order which is based on the topological properties of states [3]; the confinement and deconfinement states can be clarified from the ground state degeneracy at $T = 0$ [4]. In the topological order, there are no classical order parameters which can be used in the Ginzburg-Landau analysis and thus the spontaneous symmetry breaking is not necessary; the ground state degeneracy in the compactified spaces plays a crucial role to clarify the topologically ordered and disordered states. Unfortunately, the ground state degeneracy is difficult to apply to the thermal system and thus it is not straightforward to investigate the thermal confinement-deconfinement transition by using the topological order. Recently, the topology of the spacial structure of configurations has been used to investigate the confinement-deconfinement nature of QCD via the persistent homology [5, 6]. This approach has relation with the center clustering structure and is expected to provide additional information of the confinement-deconfinement nature via the spacial structure of configurations.

There are several studies which employ the persistent homology analysis to investigate the phase transitions [7–10]. In these studies, the authors try to detect and investigate the phase transition appearing in the condensed matter system. In addition, there are some other applications in several research fields such as the string landscape and the structure of the universe [11, 12]. We work in the same direction with Refs. [7–10]. This paper is organized as follows. In the next section 2, we explain the formulation of the Potts model. Numerical results are shown in Sec. 3, and Sec. 4 is devoted to the summary.

2. Formulation

In this study, we employ the Potts model with a suitable constructed external magnetic field. First, we explain the formulation of the Potts model and after we show details of the persistent homology analysis.

2.1 Potts model

The energy of the standard Potts model with the external magnetic field is defined as

$$E = -\kappa \sum_{\mathbf{x}} \sum_{\mathbf{i}} \delta_{k_{\mathbf{x}}k_{\mathbf{x}+\mathbf{i}}} - h \sum_{\mathbf{x}} k_{\mathbf{x}}, \quad (1)$$

where κ means the coupling constant, $k_{\mathbf{x}}$ mean the \mathbb{Z}_3 valued spin degrees of freedom at each site \mathbf{x} , \mathbf{i} means the three-dimensional unit vector and h is the strength of the external magnetic field. In this study, we allocate $k = -1, 0$ and 1 for the \mathbb{Z}_3 valued spin degrees of freedom. In this model, κ is treated as the temperature-like quantity.

To make the Potts model as the QCD effective model with heavy quarks, we reconstruct the external magnetic field as

$$E = -\kappa \sum_{\mathbf{x}} \sum_{\mathbf{i}} \delta_{k_{\mathbf{x}}k_{\mathbf{x}+\mathbf{i}}} - \sum_{\mathbf{x}} \left[h_- \Phi_{\mathbf{x}} + h_+ \bar{\Phi}_{\mathbf{x}} \right], \quad (2)$$

where the Polyakov loop ($\Phi_{\mathbf{x}}$), its conjugate ($\bar{\Phi}_{\mathbf{x}}$) and the external magnetic fields (h_{\mp}) are defined as

$$\Phi_{\mathbf{x}} = e^{2\pi i k_{\mathbf{x}}/3}, \quad \bar{\Phi}_{\mathbf{x}} = e^{-2\pi i k_{\mathbf{x}}/3}, \quad h_{\mp} = e^{-\beta(M \mp \mu)}, \quad (3)$$

here $\beta = 1/T$ is the inverse temperature, M is the quark mass and μ denotes the chemical potential; see Refs. [13–15] for details of derivation about the present form of the external magnetic field.

However, the above Potts model has the sign problem and thus we here consider following setup [6];

$$\begin{aligned} E_{\text{iso}} &= -\kappa \sum_{\mathbf{x}, \mathbf{i}} \delta_{k_{\mathbf{x}}k_{\mathbf{x}+\mathbf{i}}} - \sum_{\mathbf{x}} \left[(h_+ \Phi_{\mathbf{x}} + h_- \bar{\Phi}_{\mathbf{x}}) + (h_- \Phi_{\mathbf{x}} + h_+ \bar{\Phi}_{\mathbf{x}}) \right] \\ &= -\kappa \sum_{\mathbf{x}, \mathbf{i}} \delta_{k_{\mathbf{x}}k_{\mathbf{x}+\mathbf{i}}} - \sum_{\mathbf{x}} \left[h_+ (\Phi_{\mathbf{x}} + \bar{\Phi}_{\mathbf{x}}) + h_- (\Phi_{\mathbf{x}} + \bar{\Phi}_{\mathbf{x}}) \right] \\ &= -\kappa \sum_{\mathbf{x}, \mathbf{i}} \delta_{k_{\mathbf{x}}k_{\mathbf{x}+\mathbf{i}}} - N_f \sum_{\mathbf{x}} \left[(h_+ + h_-) \cos(\Phi_{\mathbf{x}}) \right] \in \mathbb{R}. \end{aligned} \quad (4)$$

where $N_f = 2$ is the number of flavors. This setup is corresponding to the system with the isospin chemical potential and thus there is no sign problem. Actually, there are the discussions that the isospin chemical potential and the real quark chemical potential has the direct relation at least in the large N_c limit. Therefore, we can consider the isospin chemical potential is a good laboratory to investigate the system with real quark chemical potential. Below, we call the Potts model (4) as the QCD-like Potts model. In the QCD-like Potts model, κ is treated as the temperature-like quantity to control the behavior of the Polyakov loop.

The global information of the system can be seen from the spacial-averaged Polyakov-loop with the configuration average defined as

$$\Phi = \left\langle \frac{1}{N} \sum_{\mathbf{x}} \Phi_{\mathbf{x}} \right\rangle, \quad (5)$$

where N is the total number of sites and $\langle \cdots \rangle$ means the configuration averaging. Unfortunately, this quantity can not show the spacial structure of the system because the spacial averaging is

imposed. To overcome this point, we will consider the persistent homology as explained in the next section.

We here summarize our numerical setup. The actual Potts spin configurations are obtained by using the Metropolis method with $\beta = 1/T = 1$ and $M = 10$ for the $L^3 = 30^3$ squared lattice system. The one-spin flipping probability distribution is set to $\mathcal{P} = \exp(-\beta\Delta E)$ where ΔE is the energy difference in one spin flipping process. We generates 1000 spin configurations for each L^3 updation (1 Monte-Carlo step) after the thermalization. The following figures are taken from our paper [6]. Statistical errors are estimated by using the Jack-knife method.

2.2 Persistent homology

One of ways to investigate the topology of the spacial structure of data is the persistent homology analysis. The standard way to investigate the persistent homology is using the point cloud via the filtration. We first divide the spin configuration to three data sets, namely the data set with $k = -1, 0$ and 1 spins; this means that if sites have $k = i$ spin, where $i = -1, 0, 1$, such sites are "on" and the others are set to "OFF", to each data set. After this procedure, we obtain the spacial nontrivial structure which respects the spin degrees of freedom. Then, we can consider the filtration as explained below;

- Consider balls whose centre is set to the "ON" cites for each data point (point cloud).
- The radius r for each ball is enlarged with increasing time (filtration).
- When the time passes sufficiently, the balls are started to overlap. We call this time when the hole of the overlapped balls appear as *birth time*, t_B
- After overlapping, the hole is finally vanished with increasing time. We call this time as "death time", t_D . Therefore, we have $t_B < t_D$.

Unfortunately, the above strict filtration is numerically difficult and thus the alpha complex is usually employed to approximate it. In this study, we use the alpha complex for the filtration process; see Ref. [5] for details as an example.

To see the global information of the system via the persistent homology analysis, the averaged ratio of t_B and t_D defined as

$$R = \left\langle \frac{1}{N_h} \sum_n \frac{t_{n,D}}{t_{n,B}} \right\rangle, \quad (6)$$

where the summation runs for all holes, n assigns each hole and N_h means the total number of holes for one configuration. On the other hand, the maximum value of the ratio

$$R_{\max} = \left\langle \max \left(\frac{t_D}{t_B} \right) \right\rangle, \quad (7)$$

can rather responsible for the local information of the system because it is usually expected that data appearing on the diagonal line of the persistent diagram can have the nontrivial spacial structure.

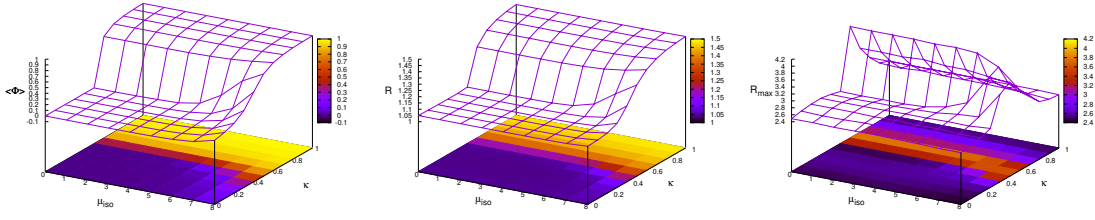


Figure 1: Panels from the left to the right show the mean value of the spatial averaged Polyakov-loop, the averaged birth-death time ratio and the maximum birth-death ratio on the $\mu_{\text{iso}}\text{-}\kappa$ plane, respectively. Statistical errors are small and thus we do not show them here.

3. Numerical results

Panels from the right to left in Fig. 1 show the κ -dependence of the spatial averaged Polyakov-loop (Φ), the averaged birth-death time ratio (R_{ave}) and the maximum birth-death ratio (R_{max}), respectively. We can clearly see that Φ and R shares the same tendency, but Φ and R_{max} does not. This means that the relatively small hole structures which are perfectly neglected in the computation of R_{max} are responsible to the global structure of the system as the same with Φ . On the other hand, R_{max} shows the more complicated behavior than R .

Figure 2 shows the snapshot of the center panel of Fig. 1. There is the valley structure before the peak structure at small μ_{iso} . This may indicate the existence of the first-order transition and it may be responsible to the clustering structure. Unfortunately, the present model does not have the violation of the spectral positivity and thus clear inhomogeneities are not expected to be observed after the configuration averaging procedure. We will discuss it in the future.

New results of the present study are that we can clarify the roles of the small and large spatial hole structures appearing in each configuration via the point cloud approach to the confinement-deconfinement phase transition. From above results, we can expect that the persistent homology can surely detect the spatial structure of the configuration, and thus we can expect that it is useful to explore the nontrivial spatial structure appearing in dense QCD.

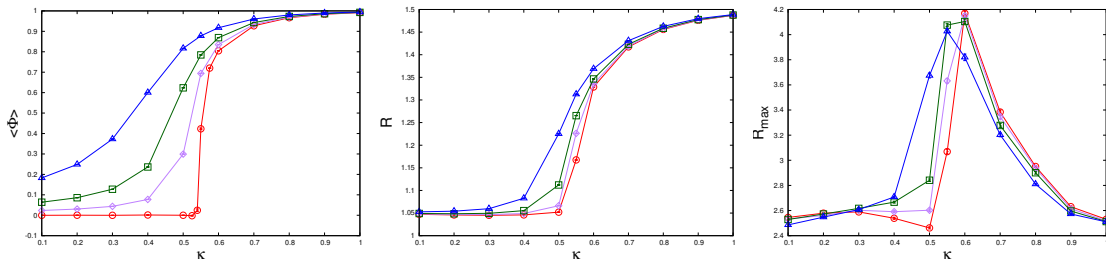


Figure 2: Panels from the left to the right show the κ -dependence of the spatial averaged Polyakov-loop, the averaged birth-death time ratio and the maximum birth-death ratio, respectively. The open circle, diamond, square and triangle symbols are results with $\mu_{\text{iso}} = 0, 6, 7$ and 8 , respectively. Lines are just eye guides.

4. Summary

In this study, we have employed the persistent homology analysis to investigate the confinement-deconfinement nature of QCD by using the QCD effective model with heavy quarks; i.e. the Potts model with a suitably constructed external magnetic field. Actually, we introduce the isospin chemical potential to investigate the dense system.

We have clarified that the averaged the birth-death time ratio is clearly matched with the behavior of the spatial averaged Polyakov-loop. Thus, this quantity is only responsible for the bulk properties of the system. This means that the spatial small hole structure plays an important role in the bulk properties. On the other hand, the maximum birth-death time ratio has more information than the bulk properties.

References

- [1] Larry D. McLerran and Benjamin Svetitsky. Quark Liberation at High Temperature: A Monte Carlo Study of SU(2) Gauge Theory. *Phys. Rev. D*, 24:450, 1981.
- [2] Kenji Fukushima, Toru Kojo, and Wolfram Weise. Hard-core deconfinement and soft-surface delocalization from nuclear to quark matter. *Phys. Rev. D*, 102(9):096017, 2020.
- [3] X. G. Wen. Topological Order in Rigid States. *Int.J.Mod.Phys.*, B4:239, 1990.
- [4] Masatoshi Sato. Topological discrete algebra, ground state degeneracy, and quark confinement in QCD. *Phys.Rev.*, D77:045013, 2008.
- [5] Takehiro Hirakida, Kouji Kashiwa, Junpei Sugano, Junichi Takahashi, Hiroaki Kouno, and Masanobu Yahiro. Persistent homology analysis of deconfinement transition in effective Polyakov-line model. *Int. J. Mod. Phys. A*, 35(10):2050049, 2020.
- [6] Kouji Kashiwa, Takehiro Hirakida, and Hiroaki Kouno. Persistent homology analysis for dense QCD effective model with heavy quarks. *arXiv:2103.12554*, 2021.
- [7] Irene Donato, Matteo Gori, Marco Pettini, Giovanni Petri, Sarah De Nigris, Roberto Franzosi, and Francesco Vaccarino. Persistent homology analysis of phase transitions. *Physical Review E*, 93(5):052138, 2016.
- [8] Bart Olsthoorn, Johan Hellsvik, and Alexander V Balatsky. Finding hidden order in spin models with persistent homology. *Physical Review Research*, 2(4):043308, 2020.
- [9] Alex Cole, Gregory J Loges, and Gary Shiu. Quantitative and interpretable order parameters for phase transitions from persistent homology. *arXiv:2009.14231*, 2020.
- [10] Quoc Hoan Tran, Mark Chen, and Yoshihiko Hasegawa. Topological persistence machine of phase transitions. *Physical Review E*, 103(5):052127, 2021.
- [11] Willem Elbers and Rien van de Weygaert. Persistent topology of the reionization bubble network – I. Formalism and phenomenology. *Mon. Not. Roy. Astron. Soc.*, 486(2):1523–1538, 2019.

- [12] Alex Cole and Gary Shiu. Topological Data Analysis for the String Landscape. *JHEP*, 03:054, 2019.
- [13] Mark G. Alford, S. Chandrasekharan, J. Cox, and U. J. Wiese. Solution of the complex action problem in the Potts model for dense QCD. *Nucl. Phys.*, B602:61–86, 2001.
- [14] Seyong Kim, Ph. de Forcrand, S. Kratochvila, and T. Takaishi. The 3-state Potts model as a heavy quark finite density laboratory. *PoS*, LAT2005:166, 2006.
- [15] Kouji Kashiwa and Hiroaki Kouno. Information theoretical view of QCD effective model with heavy quarks. *Phys. Rev. D*, 103(1):014014, 2021.